Prev. Nutr. Food Sci. 2023;28(3):255-262
https://doi.org/10.3746/pnf.2023.28.3.255
ISSN 2287-8602

Effects of Mealworm Fermentation Extract and Soy Protein Mix Ratio on Hepatic Glucose and Lipid Metabolism in Obese-Induced Mice

Ra-Yeong Choi[1] and Mi-Kyung Lee[2]

[1]Department of Agricultural Biology, National Institution of Agricultural Sciences, Rural Development Administration, Jeonbuk 55365, Korea
[2]Department of Food and Nutrition, Sunchon National University, Jeonnam 57922, Korea

ABSTRACT: Previous studies found that mealworm fermentation extract (TMP) reduced alcoholic hepatic steatogenesis. This study examined how the ratio of TMP and soy protein (SP) mix affected glucose and lipid metabolism in obese mice given a high-fat diet (HFD). Mice were given HFD supplemented with 100% SP or the following three ratios of TMP and SP mix for 12 weeks: 20% (S4T1), 40% (S3T2), and 60% (S2T3) TMP. When compared to the SP group, the S2T3 group had considerably lower body weight gain and food consumption. When compared to the SP group, the S2T3 group had slightly lower blood insulin and leptin levels, as well as a lower homeostasis model assessment of insulin resistance score. The use of TMP instead of SP reduced the size of epididymal adipose tissue cells. An increase in the extent of substitution of SP with TMP inhibited the gene expression of hepatic fructolysis/gluconeogenesis (*KHK*, *ALDOB*, *DLD*, and *FBP1)*, lipogenesis (*FAS*, *SCD1*, *CD36*, and *DGAT2*), and its transcriptional factors (*PPARγ* and *ChREBP*). Furthermore, the S2T3 group dramatically reduced the expression of hepatic genes implicated in endoplasmic reticulum stress (*PDI*) and antioxidant defense (*SOD1*). The 60% TMP mix, in particular, reduced the expression of hepatic glucose and lipid metabolism-related genes in HFD-fed mice. The manufacturing of functional processed goods may be accomplished by combining SP and TMP in a 2:3 ratio.

Keywords: fatty liver, high-fat diet, lipid metabolism, soybean protein, *Tenebrio molitor*

INTRODUCTION

Obesity and its associated comorbidities, such as type 2 diabetes, cardiovascular disease, hypertension, and cancer have increased worldwide (Drummen et al., 2018). Carbohydrate response element-binding protein (ChREBP) plays a crucial role in the development of non-alcoholic fatty liver disease (NAFLD), glucose intolerance, dyslipidemia and cancer, and controls the transcription of genes involved in glucose and lipid metabolism, impacting these clinical diseases (Iizuka, 2017). Controlling dietary protein consumption has recently been identified as a viable method for reducing obesity (Ijaz et al., 2018). A prior meta-analysis found that an isocaloric high-protein diet is superior to a conventional protein diet in terms of weight reduction, body composition, and management of resting energy expenditure (Wycherley et al., 2012). Indeed, casein has been employed as the only protein component in the majority of commercially purified diets for obesity (Choi et al., 2021). Soy protein (SP) is classified as a complete protein as it includes the majority of the necessary amino acids present in animal protein and is approximately similar to high-biological-value animal protein (Velasquez and Bhathena, 2007). Torre-Villalvazo et al. (2008) found that long-term (180-day) SP treatment had positive effects on the liver and adipose tissue in rats, even when given a high-fat diet (HFD).

Tenebrio molitor larva (mealworm) is a nutritious edible insect that provides essential amino acids, polyunsaturated fatty acids, trace elements, and vitamins (Feng, 2018). Gessner et al. (2019) reported that isonitrogenous substitution of 50% and 100% of casein with mealworm meal had lipid-lowering benefits in a hyperlipidemic rat model. The purpose of this study was to see how different ratios of mealworm fermentation extract (TMP) and SP mix (20, 40, or 60% TMP) affected hepatic glucose and lipid metabolism-related gene expression in HFD-induced obese mice.

Received 27 March 2023; Revised 30 May 2023; Accepted 20 June 2023; Published online 30 September 2023
Correspondence to Mi-Kyung Lee, E-mail: leemk@scnu.ac.kr

MATERIALS AND METHODS

Animals and diets

Male C57BL/6N mice aged 4 weeks (n=40) were bought from Orient Bio Inc., and kept under normal circumstances (22±2°C, 50±5% humidity, and a 12-h light/dark cycle). The Sunchon National University's Institutional Animal Care and Use Committee (SCNU_IACUC_2020-08) gave its approval to the protocol. The mice were divided into 4 groups of 10 mice each after a week of acclimatization. The mice were given HFD supplemented with SP (Shandong Yuxin Bio-Tech Co., Ltd.) as the control or three concentrations of TMP (20, 40, and 60%) and SP mix (S4T1, S3T2, and S2T3), each of which included 20% protein sources, in three different ratios. Table 1 contains a list of the experimental diets and their ingredients. The mice have limitless access to food and water at all times. Three times a week, the diet was modified, and once a week, the body weight was recorded. The overnight-starved mice were put to death with inhalation after the 12-week trial, and blood was taken from the inferior vena cava as described in our prior work (Ham et al., 2021). In preparation for further examination, the liver and white adipose tissues (WAT) were extracted and kept at −80°C. For histological investigation, certain tissue samples were fixed in 10% neutral buffered formalin. According to the preceding instructions, the TMP was extracted (Choi et al., 2020a). In the yeast extract–peptone–dextrose medium, defatted and freeze-dried mealworm powder was used to replace peptone. After being infused into the broth, the *Saccharomyces cerevisiae* strain (KCTC 17299) from the Korean Cell Line Bank was incubated for 72 h at 32±3°C. The yeast/mealworm fermentation broth (1 L) was then extracted with 1 L of fermented alcohol at a 70% concentration. The sample extractions underwent filtering, evaporation, and freeze-drying.

Table 1. Dietary composition in experiments[1)]

Ingredients (%)	SP	S4T1	S3T2	S2T3
SP	20.0	16.0	12.0	8.0
TMP	−	4.0	8.0	12.0
DL-methionine	0.3	0.3	0.3	0.3
Choline bitartrate	0.2	0.2	0.2	0.2
Corn starch	34.0	34.0	34.0	34.0
Sucrose	15.0	15.0	15.0	15.0
Cellulose	5.0	5.0	5.0	5.0
Corn oil	3.0	3.0	3.0	3.0
Lard	18.0	18.0	18.0	18.0
Mineral mixture[2)]	3.5	3.5	3.5	3.5
Vitamin mixture[3)]	1.0	1.0	1.0	1.0

[1)]Experimental diets were adjusted ratio for protein contents.
[2)]Mineral mixture according to AIN-76.
[3)]Vitamin mixture according to AIN-76.
SP, soy protein; TMP, mealworm fermentation extract.

Serum biochemical assays

Using an assay kit, the glucose level was determined (Asan Pharmaceutical Co., Ltd.). Enzyme-linked immunosorbent assay kits from R&D Systems, Inc. and Morinaga Institute of Biological Science, Inc. were used to measure the levels of leptin and insulin, respectively. The equation fasting insulin (μIU/mL)×fasting glucose (mmol/L)/22.5 was used to calculate the homeostasis model assessment of insulin resistance (HOMA-IR).

Histological analysis

Hematoxylin and eosin (H&E) staining was performed on the paraffin-embedded fixed liver and epididymal WAT. Oil Red O was used to stain the liver slices. A 200× optical microscope was used to magnify the tiny pictures for observation.

RNA isolation and reverse transcription quantitative polymerase chain reaction (RT-qPCR) analysis

The total RNA was isolated using the TRIzol reagent (Invitrogen, Thermo Fisher Scientific, Inc.). RNA content was quantified using a NanoDrop 2000 spectrophotometer (Thermo Fisher Scientific, Inc.). Complementary DNA synthesis was performed using a ReverTra Ace qPCR RT master mix (Toyobo). The RT-qPCR analysis was conducted using the CFX96 Touch™ real-time PCR detection system (Bio-Rad Laboratories, Inc.) with an SYBR green PCR kit (Qiagen). The primer details can be found in Table 2.

Statistical analysis

Statistical analysis was performed using IBM SPSS software (version 20, IBM Corp.). The data are presented as mean±standard error. One-way ANOVA was utilized to determine significant differences among the groups, followed by Tukey's test. Statistical significance was considered at a threshold of $P<0.05$.

RESULTS

Body weight, food intake, and insulin resistance index

There were no significant changes in weekly body weights for the first 9 weeks. However, after 10 weeks on the experimental diet, the body weights in the S2T3 group showed a trend toward being lower compared to the SP, S4T1, and S3T2 groups (Table 3). By the 12th week, the S2T3 group exhibited a significantly reduced body weight gain compared to the other groups (Table 3). Furthermore, the S2T3 group demonstrated a significant decrease in food intake compared to the SP group (Table 3). Serum glucose levels did not show significant statistical changes among the four groups (Table 3). Nevertheless, the serum insulin and leptin levels, as well as the HOMA-

Table 2. Primer sequences for quantitative real-time polymerase chain reaction based on reverse transcription

Gene	Name	Forward/reverse (5′-3′)
ALDOB	Fructose bisphosphate aldolase B	GCTGTGTTGAGGATTGCTGA/TAGACAGCAGCCAGGACCTT
CD36	Cluster of differentiation 36	GCTGTCAGGCGTCAGGATAA/TGGCTTCAGGGAGACTGTTG
ChREBP	Carbohydrate-response element-binding protein	CTGGGGACCTAAACAGGAGC/GAAGCCACCCTATAGCTCCC
DGAT2	Diacylglycerol O-acyltransferase 2	CTGGCTGATAGCTGCTCTCTACTTG/TGTGATCTCCTGCCACCTTTC
DLD	Dihydrolipoyl dehydrogenase	CCTTGTAGCTACGGGCTCAG/CCCACATGACCCAAAAATTC
FAS	Fatty acid synthase	TTGGAGCTAAGGCATGGTGG/GCAGTTGTCCTCTGGATGCT
FBP1	Fructose-1,6-bisphosphatase 1	GTCTGTTTCGATCCCCTTGA/GTCCAGCATGAAGCAGTTGA
GAPDH	Glyceraldehyde-3-phosphate dehydrogenase	AAGGTCATCCCAGAGCTGAA/CTGCTTCACCACCTTCTTGA
KHK	Ketohexokinase	TCGAGTGAAGAAAGGGGCTA/CCTTCGAGAGGCTGAAGATG
PAP	Phosphatidate phosphatase 1	GGGTTCTACTGTGGAGATGA/TGACAGTAGCTGTGATGATGA
PDI	Protein disulfide isomerase	TATGATGGGCCTAGGACTGC/TGCTGGCTGCTTTTAGGAAT
PPARγ	Peroxisome proliferator-activated receptor gamma	TCGCTGATGCACTGCCTATG/GAGAGGTCCACAGAGCTGAT
SCD1	Stearoyl-CoA desaturase	TTCTTCATCGACTGCATGGC/ACTCAGAAGCCCAAAGCTCAG
SOD1	Superoxide dismutase 1	CCAGTGCAGGACCTCATTTT/TTGTTTCTCATGGACCACCA
SREBP-1c	Sterol regulatory element-binding protein 1c	AACCTCATCCGCCACCTG/TGGTAGACAACAGCCGCATC

Table 3. Obese mice given high-fat diets with a TMP/SP mix had different body weights, food intakes, serum glucose, insulin, and leptin levels, and HOMA-IR

	SP	S4T1	S3T2	S2T3
Body weights (g)				
0 week	19.20±0.33	19.53±0.24	19.53±0.24	19.54±0.24
3 week	26.07±0.26	26.19±0.57	25.85±0.29	25.40±0.38
6 week	31.79±0.51	32.67±0.98	32.16±0.55	31.22±0.63
9 week	37.81±0.71	38.83±1.22	37.32±0.79	35.17±0.71
10 week	39.49±0.76^{ab}	40.66±1.27^{b}	39.25±0.95^{ab}	36.65±0.78^{a}
11 week	40.65±0.82^{ab}	41.71±1.23^{b}	40.77±0.94^{ab}	37.67±0.80^{a}
12 week	41.23±0.82^{ab}	42.41±1.16^{b}	41.92±0.94^{ab}	38.41±0.82^{a}
Body weight gain (g)	22.02±0.59^{b}	22.87±1.04^{b}	22.39±0.77^{b}	18.93±0.77^{a}
Food intakes (g/d)	3.93±0.05^{b}	3.71±0.05^{ab}	3.70±0.08^{ab}	3.45±0.07^{a}
Serum glucose (mmol/L)	14.10±1.63	14.96±1.15	12.99±1.03	10.52±0.69
Serum insulin (μIU/mL)	100.53±26.93^{ab}	153.37±33.27^{b}	132.20±21.30^{ab}	51.27±8.70^{a}
Serum leptin (ng/mL)	7.23±1.23^{ab}	8.57±1.04^{b}	7.58±0.80^{ab}	4.46±0.78^{a}
HOMA-IR	68.18±21.59^{ab}	97.57±20.04^{b}	79.84±17.00^{ab}	25.49±5.45^{a}

The data are shown as mean±SE. Means with distinct letters (a,b) in a row show statistically significant differences between groups.
TMP, mealworm fermentation extract; SP, soy protein; HOMA-IR, homeostasis model assessment of insulin resistance.

IR index, tended to be reduced in the S2T3 group compared to the SP group (Table 3).

Morphological changes in the adipose tissue and liver

The histological examination of epididymal WAT stained with H&E revealed that the adipocyte size was smaller in proportion to the substitution ratio of TMP replacing SP (Fig. 1). In the histological analysis of hepatic tissues using H&E staining, the SP group exhibited a noticeable increase in fat vacuoles, while the TMP-replacement groups (S4T1, S3T2, and S2T3) showed fewer lipid droplets (Fig. 1). The presence of Oil Red O-positive lipid droplets in the SP group was observed throughout the liver, whereas increasing the TMP-replacement ratio resulted in reduced lipid accumulation compared to the SP group (Fig. 1).

Changes in expression of gene controlling hepatic fructolysis/gluconeogenesis

Fig. 2 demonstrates that the gene expression of *KHK* and *ALDOB* was significantly suppressed when TMP substitution levels exceeded 60%. Similarly, the gene expression of *DLD* and *FBP1* was down-regulated with increasing substitution of SP by TMP (Fig. 2). Notably, these four genes exhibited a pronounced down-regulation in the S2T3 group compared to the SP group.

Changes in expression of gene controlling hepatic lipogenesis

In relation to fatty acid synthesis, the gene expression of *FAS* and *SCD1* was significantly down-regulated at TMP-replacement levels exceeding 40% and 60%, respectively, compared to the SP group (Fig. 3). In addition, the mRNA expression of the fatty acid uptake-related gene *CD36* was

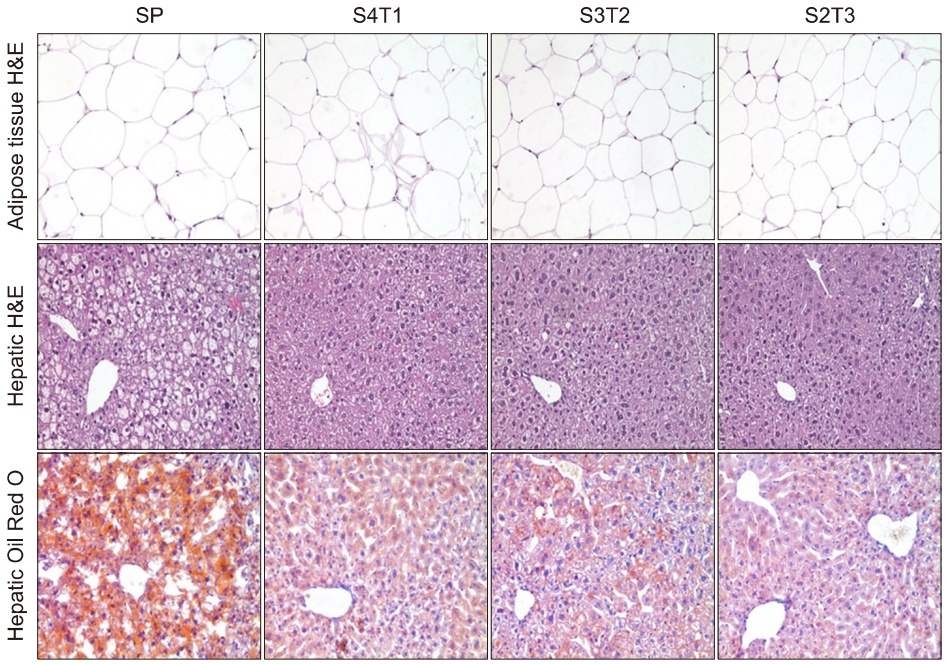

Fig. 1. Histological appearance of epididymal white adipose tissue and liver in obese mice fed high-fat diets with varying ratios of mealworm fermentation extract and soy protein (SP) mix. Magnification: 200×. H&E, hematoxylin and eosin.

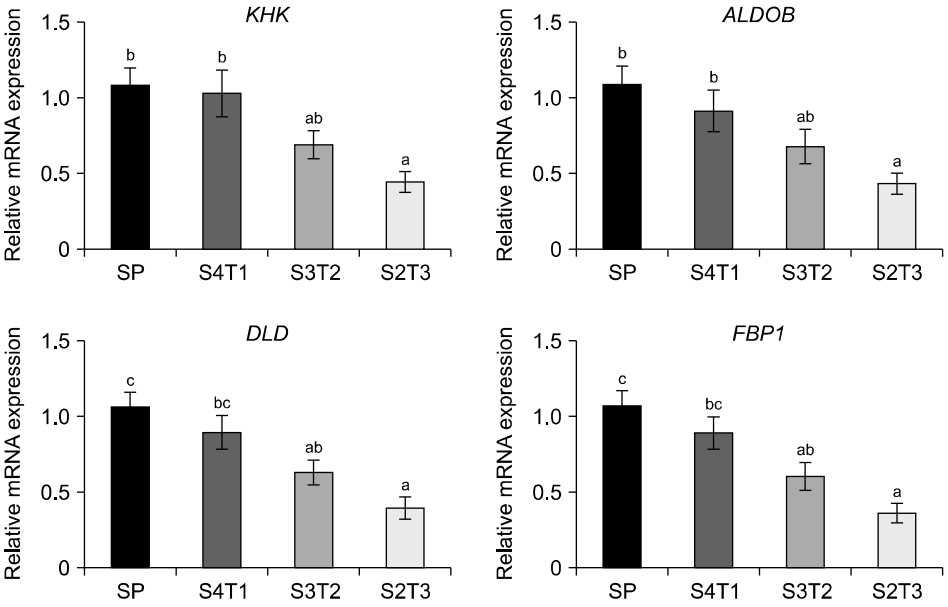

Fig. 2. Gene expression related to hepatic fructolysis/gluconeogenesis in obese mice fed high-fat diets with varying ratios of mealworm fermentation extract and soy protein (SP) mix. Data are presented as mean±SE. Different letters (a-c) above the bars indicate significant differences among the groups.

significantly decreased in the S3T2 and S2T3 groups compared to the SP group (Fig. 3). While the expression of *PAP* was lower in the TMP-replacement groups, no significant differences were observed (Fig. 3). Furthermore, the mRNA levels of the triglyceride synthesis gene *DGAT2* were significantly down-regulated in the S4T1, S3T2, and S2T3 groups compared to the SP group (Fig. 3).

Changes in expression of hepatic transcription factor genes

The mRNA levels of glucose and lipid metabolism-related transcription factors were measured (Fig. 4). The *PPARγ* gene expression in the S2T3 group was significantly lower than in the SP group. As the addition ratio of TMP increased, the *ChREBP* gene expression in the TMP-replacement groups was down-regulated compared with the SP group. The TMP replacement did not affect the *SREBP-1c* gene expression.

Changes in expression of hepatic endoplasmic reticulum (ER) stress and antioxidant gene expression

Major indicators of ER-related stress and antioxidants, respectively, are *PDI* and *SOD1*. In a dose-dependent manner, the expression levels of the *PDI* and *SOD1* genes were reduced in the TMP-replacement groups in comparison to the SP group (Fig. 5).

DISCUSSION

We previously reported that glutamic acid, leucine, and

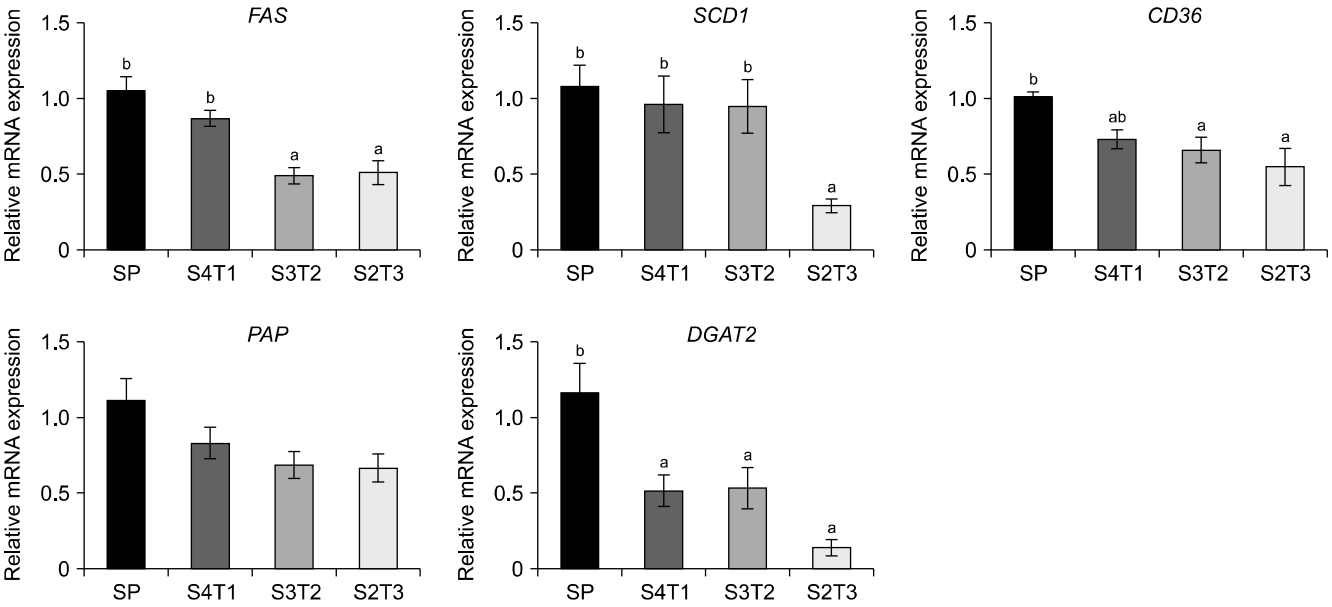

Fig. 3. Gene expression related to hepatic lipogenesis in obese mice fed high-fat diets with varying ratios of mealworm fermentation extract and soy protein (SP) mix. Data are presented as mean±SE. Different letters (a,b) above the bars indicate significant differences among the groups.

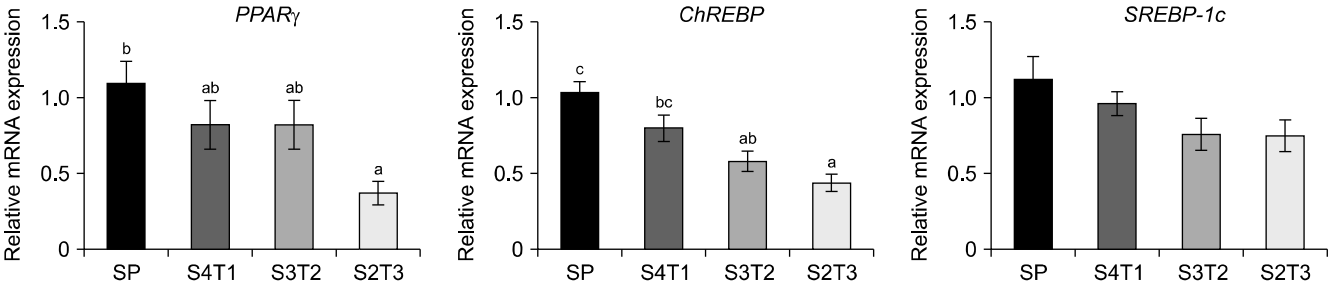

Fig. 4. Gene expression of hepatic transcription factors in obese mice fed high-fat diets with varying ratios of mealworm fermentation extract and soy protein (SP) mix. Data are presented as mean±SE. Different letters (a-c) above the bars indicate significant differences among the groups.

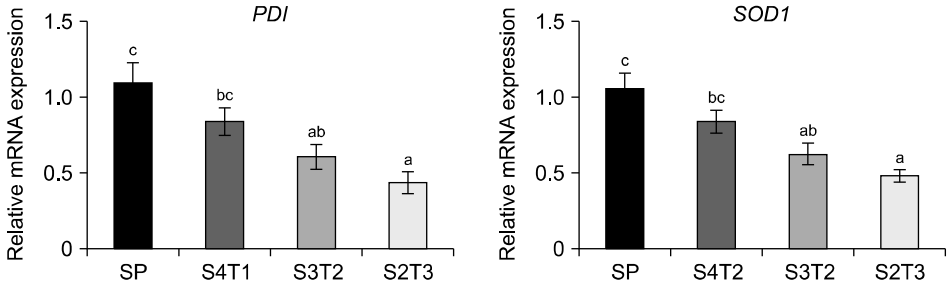

Fig. 5. Gene expression of hepatic endoplasmic reticulum stress and antioxidant-related genes in obese mice fed high-fat diets with varying ratios of mealworm fermentation extract and soy protein (SP) mix. Data are presented as mean±SE. Different letters (a-c) above the bars indicate significant differences among the groups.

alanine were the most prevalent amino acids in TMP (Choi et al., 2020b). Zhang et al. (2007) discovered that dietary leucine supplementation decreases HFD-induced hypercholesterolemia, hyperglycemia, and adiposity in rodents. L-alanine or L-arginine administration has been found to reduce obesity and glucose intolerance in mice induced to be obese by monosodium glutamate (Araujo et al., 2017). Glutamine supplementation decreases adipose mass and enhances insulin sensitivity in HFD-fed Wistar rodents, according to Abboud et al. (2019). The present study demonstrated that as the ratio of TMP to SP in the mixture increased, the expression of genes implicated in *ChREBP*-mediated glucose and lipid metabolism improved in NAFLD. Specifically, the 60% ratio by TMP (S2T3 group) substantially decreased the *KHK* and *ALDOB* genes relative to the SP group. Shepherd et al.

(2020) reported that KHK catalyzes fructose into fructose-1-phosphate, which is then cleaved by ALDOB into glyceraldehyde and dihydroxyacetone-phosphate. Triokinase converts glyceraldehyde to glyceraldehyde 3-phosphate, which is then converted to glucose by gluconeogenesis or further metabolized into acetyl-CoA, resulting in lipogenesis (Lee and Cha, 2018). In addition to being intermediates of fructolysis and glycolysis, triose phosphates are also intermediates of glyceroneogenesis and gluconeogenesis (Masania et al., 2016). Moreover, TMP replacement inhibited the expression of the *FBP1* gene relative to SP. FBP1 is a rate-limiting enzyme in hepatic gluconeogenesis that is increased by obesity and dietary fat intake (Visinoni et al., 2012). Thus, TMP can inhibit fructolysis/gluconeogenesis in obese rodents induced by a HFD. Gutierrez et al. (2021) have reported that *KHK* inhibition prevents fructose metabolism in the liver, resulting in suppressed *ChREBP*, insulin resistance, and *de novo* lipogenesis (DNL). ChREBP and SREBP-1c are important transcriptional regulators in liver X receptor-mediated hepatic lipogenesis through the upregulation of fatty acid synthase and acetyl-CoA carboxylase (Xu et al., 2013). ChREBP is a glucose-responsive factor that is essential for fructose-induced lipogenesis and gluconeogenesis in the liver (Iizuka et al., 2004; Ma et al., 2006; Shin et al., 2016; Lee and Cha, 2018). Hepatic deletion or suppression of *ChREBP* decreases the expression of enzymes involved in glycolysis, gluconeogenesis, lipogenesis, and very low-density lipoprotein packaging and secretion, which protects against obesity and insulin resistance (Katz et al., 2021). In this study, the dose-dependent replacement of TMP decreased *ChREBP* gene expression but not *SREBP-1c* gene expression relative to SP. In addition, the *ChREBP*-downstream genes *FAS* and *DGAT2* were substantially lower in the TMP group (more than 40% for *FAS* and more than 20% for *DGAT2*) than in the SP group. Thus, TMP appears to inhibit *ChREBP*-mediated fatty acid and triglyceride synthesis to suppress fructose-induced lipogenesis and gluconeogenesis.

The present study also observed a significant decrease in *PPARγ* expression in the S2T3 group (60% TMP-replacement group) compared to the SP group. PPARγ plays a crucial role in regulating lipid metabolism, targeting genes involved in DNL and free fatty acid uptake (Skat-Rørdam et al., 2019). It also modulates adipogenic genes such as adipocyte fatty acid-binding protein and *CD36*, promoting free fatty acid uptake. Increased hepatic *PPARγ* expression has been observed in patients with NAFLD (Skat-Rørdam et al., 2019). Moreover, Matsusue et al. (2014) reported that liver-specific knockout of *PPARγ* in *ob/ob* mice significantly reduced hepatic triglyceride content compared to control mice. In addition, the expression of the *SCD1* gene was down-regulated in the S2T3 group compared to the SP group. SCD1 is an enzyme involved in lipogenesis, converting saturated fatty acids to monounsaturated fatty acids, and is encoded by the *SCD1* gene, downstream of the *PPARγ* and *ChREBP* signaling pathways (Tao et al., 2021). Furthermore, histological observations revealed an increase in hepatic lipid droplets and vacuolization in the SP group, while the TMP-replacement groups showed a reduction in lipid droplets in the liver. These findings indicate that the substitution of 60% TMP for SP suppresses hepatic fatty acid uptake and lipogenic genes in HFD-induced obese mice by down-regulating the *ChREBP/PPARγ* pathway.

In contrast, the present investigation demonstrated that TMP replacement decreased *DLD* and *SOD1* expression relative to SP. During glucose metabolism and mitochondrial adenosine triphosphate production, the enzyme DLD participates in the decarboxylation of pyruvate to form acetyl-CoA. DLD can either promote or suppress reactive oxygen species (ROS) depending on pathophysiological conditions (Chen et al., 2002; Yan et al., 2008; Ambrus et al., 2011; Yan et al., 2013; Quinlan et al., 2014; Yang et al., 2019). Yang et al. (2019) reported that the inhibition of *DLD* resulted in an antioxidant response to oxidative stress in stroke injuries. Under aerobic conditions, SOD inhibits iron mobilization from ferritin by DLD (Bando and Aki, 1990). According to a previous study (Ashraf and Sheikh, 2015), ROS production is one of the main mechanisms for the progression of steatosis during ER stress. ER is predominantly involved in protein folding and post-translational modification. The PDI family of enzymes and other oxidoreductases, which contribute to the generation of ROS, mediate the formation of the disulfide bond in proteins (Zhang et al., 2019). Compared to SP, the TMP replacement inhibited the expression of the *PDI* gene in the current study. Although the exact mechanism by which TMP is involved in oxidative and ER stress is unknown, it has been demonstrated that partial replacement of SP with TMP reduces oxidative and ER stress markers. Through the regulation of ER stress, antioxidant defense, fructolysis/gluconeogenesis, lipogenesis, and their transcriptional factors, increasing the mix ratio of TMP could reduce HFD-induced lipid accumulation in mice compared to the SP group. SP and TMP were combined in a ratio of 2:3 to improve glucose and lipid metabolism in the liver tissues of HFD-induced obese mice. This mixture ratio can be used to produce functionally processed goods.

ACKNOWLEDGEMENTS

We sincerely appreciate Suncheon Research Center for Bio Health Care for providing TMP.

FUNDING

This work was supported by the National Research Foundation of Korea (NRF) grant funded by the Korea government (MSIT) (No. NRF-2020R1A2C1009008).

AUTHOR DISCLOSURE STATEMENT

The authors declare no conflict of interest.

AUTHOR CONTRIBUTIONS

Concept and design: all authors. Analysis and interpretation: all authors. Data collection: RYC. Writing the article: all authors. Critical revision of the article: MKL. Final approval of the article: all authors. Statistical analysis: RYC. Obtained funding: MKL. Overall responsibility: all authors.

REFERENCES

Abboud KY, Reis SK, Martelli ME, Zordão OP, Tannihão F, de Souza AZZ, et al. Oral glutamine supplementation reduces obesity, pro-inflammatory markers, and improves insulin sensitivity in DIO Wistar rats and reduces waist circumference in overweight and obese humans. Nutrients. 2019. 11:536. https://doi.org/10.3390/nu11030536

Ambrus A, Torocsik B, Tretter L, Ozohanics O, Adam-Vizi V. Stimulation of reactive oxygen species generation by disease-causing mutations of lipoamide dehydrogenase. Hum Mol Genet. 2011. 20:2984-2995.

Araujo TR, Freitas IN, Vettorazzi JF, Batista TM, Santos-Silva JC, Bonfleur ML, et al. Benefits of L-alanine or L-arginine supplementation against adiposity and glucose intolerance in monosodium glutamate-induced obesity. Eur J Nutr. 2017. 56:2069-2080.

Ashraf NU, Sheikh TA. Endoplasmic reticulum stress and oxidative stress in the pathogenesis of non-alcoholic fatty liver disease. Free Radic Res. 2015. 49:1405-1418.

Bando Y, Aki K. Superoxide-mediated release of iron from ferritin by some flavoenzymes. Biochem Biophys Res Commun. 1990. 168:389-395.

Chen HJ, Chen YM, Chang CM. Lipoyl dehydrogenase catalyzes reduction of nitrated DNA and protein adducts using dihydrolipoic acid or ubiquinol as the cofactor. Chem Biol Interact. 2002. 140:199-213.

Choi BS, Daniel N, Houde VP, Ouellette A, Marcotte B, Varin TV, et al. Feeding diversified protein sources exacerbates hepatic insulin resistance *via* increased gut microbial branched-chain fatty acids and mTORC1 signaling in obese mice. Nat Commun. 2021. 12:3377. https://doi.org/10.1038/s41467-021-23782-w

Choi RY, Ham JR, Ryu HS, Lee SS, Miguel MA, Paik MJ, et al. Defatted *Tenebrio molitor* larva fermentation extract modifies steatosis, inflammation and intestinal microflora in chronic alcohol-fed rats. Nutrients. 2020a. 12:1426. https://doi.org/10.3390/nu12051426

Choi RY, Ji M, Lee MK, Paik MJ. Metabolomics study of serum from a chronic alcohol-fed rat model following administration of defatted *Tenebrio molitor* larva fermentation extract. Metabolites. 2020b. 10:436. https://doi.org/10.3390/metabo10110436

Drummen M, Tischmann L, Gatta-Cherifi B, Adam T, Westerterp-Plantenga M. Dietary protein and energy balance in relation to obesity and co-morbidities. Front Endocrinol. 2018. 9:443. https://doi.org/10.3389/fendo.2018.00443

Feng S. *Tenebrio molitor* L., entomophagy and processing into ready to use therapeutic ingredients: a review. J Nutr Health Food Eng. 2018. 8:280-285.

Gessner DK, Schwarz A, Meyer S, Wen G, Most E, Zorn H, et al. Insect meal as alternative protein source exerts pronounced lipid-lowering effects in hyperlipidemic obese Zucker rats. J Nutr. 2019. 149:566-577.

Gutierrez JA, Liu W, Perez S, Xing G, Sonnenberg G, Kou K, et al. Pharmacologic inhibition of ketohexokinase prevents fructose-induced metabolic dysfunction. Mol Metab. 2021. 48:101196. https://doi.org/10.1016/j.molmet.2021.101196

Ham JR, Choi RY, Lee Y, Lee MK. Effects of edible insect *Tenebrio molitor* larva fermentation extract as a substitute protein on hepatosteatogenesis and proteomic changes in obese mice induced by high-fat diet. Int J Mol Sci. 2021. 22:3615. https://doi.org/10.3390/ijms22073615

Iizuka K, Bruick RK, Liang G, Horton JD, Uyeda K. Deficiency of carbohydrate response element-binding protein (ChREBP) reduces lipogenesis as well as glycolysis. Proc Natl Acad Sci U S A. 2004. 101:7281-7286.

Iizuka K. The transcription factor carbohydrate-response element-binding protein (ChREBP): A possible link between metabolic disease and cancer. Biochim Biophys Acta Mol Basis Dis. 2017. 1863:474-485.

Ijaz MU, Ahmed MI, Zou X, Hussain M, Zhang M, Zhao F, et al. Beef, casein, and soy proteins differentially affect lipid metabolism, triglycerides accumulation and gut microbiota of high-fat diet-fed C57BL/6J mice. Front Microbiol. 2018. 9:2200. https://doi.org/10.3389/fmicb.2018.02200

Katz LS, Baumel-Alterzon S, Scott DK, Herman MA. Adaptive and maladaptive roles for ChREBP in the liver and pancreatic islets. J Biol Chem. 2021. 296:100623. https://doi.org/10.1016/j.jbc.2021.100623

Lee HJ, Cha JY. Recent insights into the role of ChREBP in intestinal fructose absorption and metabolism. BMB Rep. 2018. 51:429-436.

Ma L, Robinson LN, Towle HC. ChREBP*Mlx is the principal mediator of glucose-induced gene expression in the liver. J Biol Chem. 2006. 281:28721-28730.

Masania J, Malczewska-Malec M, Razny U, Goralska J, Zdzienicka A, Kiec-Wilk B, et al. Dicarbonyl stress in clinical obesity. Glycoconj J. 2016. 33:581-589. https://doi.org/10.1007/s10719-016-9692-0

Matsusue K, Aibara D, Hayafuchi R, Matsuo K, Takiguchi S, Gonzalez FJ, et al. Hepatic PPARγ and LXRα independently regulate lipid accumulation in the livers of genetically obese mice. FEBS Lett. 2014. 588:2277-2281.

Quinlan CL, Goncalves RL, Hey-Mogensen M, Yadava N, Bunik VI, Brand MD. The 2-oxoacid dehydrogenase complexes in mitochondria can produce superoxide/hydrogen peroxide at much higher rates than complex I. J Biol Chem. 2014. 289:8312-8325.

Shepherd EL, Saborano R, Northall E, Matsuda K, Ogino H, Yashiro H, et al. Ketohexokinase inhibition improves NASH by reducing fructose-induced steatosis and fibrogenesis. JHEP Rep. 2020. 3:100217. https://doi.org/10.1016/j.jhepr.2020.100217

Shin E, Bae JS, Han JY, Lee J, Jeong YS, Lee HJ, et al. Hepatic DGAT2 gene expression is regulated by the synergistic action of ChREBP and SP1 in HepG2 cells. Anim Cells Syst. 2016. 20:7-14.

Skat-Rørdam J, Højland Ipsen D, Lykkesfeldt J, Tveden-Nyborg P.

A role of peroxisome proliferator-activated receptor γ in nonalcoholic fatty liver disease. Basic Clin Pharmacol Toxicol. 2019. 124:528-537.

Tao L, Guo X, Xu M, Wang Y, Xie W, Chen H, et al. Dexmedetomidine ameliorates high-fat diet-induced nonalcoholic fatty liver disease by targeting SCD1 in obesity mice. Pharmacol Res Perspect. 2021. 9:e00700. https://doi.org/10.1002/prp2.700

Torre-Villalvazo I, Tovar AR, Ramos-Barragán VE, Cerbón-Cervantes MA, Torres N. Soy protein ameliorates metabolic abnormalities in liver and adipose tissue of rats fed a high fat diet. J Nutr. 2008. 138:462-468.

Velasquez MT, Bhathena SJ. Role of dietary soy protein in obesity. Int J Med Sci. 2007. 4:72-82.

Visinoni S, Khalid NF, Joannides CN, Shulkes A, Yim M, Whitehead J, et al. The role of liver fructose-1,6-bisphosphatase in regulating appetite and adiposity. Diabetes. 2012. 61:1122-1132.

Wycherley TP, Moran LJ, Clifton PM, Noakes M, Brinkworth GD. Effects of energy-restricted high-protein, low-fat compared with standard-protein, low-fat diets: a meta-analysis of randomized controlled trials. Am J Clin Nutr. 2012. 96:1281-1298.

Xu X, So JS, Park JG, Lee AH. Transcriptional control of hepatic lipid metabolism by SREBP and ChREBP. Semin Liver Dis. 2013. 33:301-311.

Yan LJ, Sumien N, Thangthaeng N, Forster MJ. Reversible inactivation of dihydrolipoamide dehydrogenase by mitochondrial hydrogen peroxide. Free Radic Res. 2013. 47:123-133.

Yan LJ, Thangthaeng N, Forster MJ. Changes in dihydrolipoamide dehydrogenase expression and activity during postnatal development and aging in the rat brain. Mech Ageing Dev. 2008. 129:282-290.

Yang X, Song J, Yan LJ. Chronic inhibition of mitochondrial dihydrolipoamide dehydrogenase (DLDH) as an approach to managing diabetic oxidative stress. Antioxidants. 2019. 8:32. https://doi.org/10.3390/antiox8020032

Zhang Y, Guo K, LeBlanc RE, Loh D, Schwartz GJ, Yu YH. Increasing dietary leucine intake reduces diet-induced obesity and improves glucose and cholesterol metabolism in mice *via* multimechanisms. Diabetes. 2007. 56:1647-1654.

Zhang Z, Zhang L, Zhou L, Lei Y, Zhang Y, Huang C. Redox signaling and unfolded protein response coordinate cell fate decisions under ER stress. Redox Biol. 2019. 25:101047. https://doi.org/10.1016/j.redox.2018.11.005